Proceedings of 1992 Amer. Towing Tank Conf., New Orleans, LA.

CAVITATION SCALING EXPERIMENTS WITH AXISYMMETRIC BODIES

by

Yan P. Kuhn de Chizelle*,
Steven L. Ceccio+,
Christopher E. Brennen*,
Young Shen++
* California Institute of Technology, Pasadena, California, USA
+ University of Michigan, Ann Arbor, Michigan, USA
++ David Taylor Research Center, Bethesda, Maryland, USA

ABSTRACT

Several experiments performed by Ceccio and Brennen (1991, 1989) and Kumar and Brennen (1992, 1991) have closely examined the interaction between individual cavitation bubbles and the boundary layer, as well as statistical properties of the acoustical signals produced by the bubble collapse. All of these experiments were, however, conducted in the same facility with the same headform size (5.08cm in diameter) and over a fairly narrow range of flow velocities (around 9m/s). Clearly this raises the issue of how the phenomena identified change with speed, scale and facility. The present paper describes experiments conducted in order to try to answer some of these important questions regarding the scaling of the cavitation phenomena. The experiments were conducted in the Large Cavitation Channel of the David Taylor Research Center in Memphis Tennessee, on geometrically similar Schiebe headforms which are 5.08, 25.4 and 50.8cm in diameter for speeds ranging up to 15m/s and for a range of cavitation numbers.

NOMENCLATURE

C_p	pressure coefficient, $(P - P_o)/0.5\,\rho U_o^2$
D	headform diameter
I*	dimensionless acoustic impulse
P	static local pressure
P_o	static free-stream pressure
P_v	water vapor pressure
R	bubble radius at the base
Re	Reynolds number, $U_o D/\nu$
t	time
U_o	free-stream velocity
ν	kinematic viscosity
ρ	density
σ	cavitation number, $(P_o - P_v)/0.5\,\rho U_o^2$
σ_i	inception cavitation number

1. INTRODUCTION

Questions on the scaling of cavitation have been asked for many years. The purpose of the experiments described herein is to investigate the effects of scale in the cavitation occurring on a simple axisymmetric headform. We will here focus on traveling bubble cavitation, and the interaction between the flow and the dynamics and acoustics of individual bubbles. Experiments by Ceccio and Brennen (1991) on 5.08cm diameter axisymmetric headforms had revealed a surprising complexity in the flow around single cavitation bubbles. Photographic observations showed that the bubbles have an approximately hemispherical shape and are separated from the solid surface by a thin film of liquid, as had been observed by Blake et al. (1977). The collapse phase appeared quite complex and consisted of at least three processes occurring simultaneously, namely collapse, shearing due to the velocity gradient near the surface and the rolling up of the bubbles into vortices as a natural consequence of the first two processes. It was noted that the collapse phase was dependent on the shape of the headform and the details

differed between the ITTC headform (Lindgren and Johnsson, 1966) which possessed a laminar separation and the Schiebe body (Schiebe, 1972; Meyer, Billet and Holl, 1989) which did not. Bubble fission during the collapse phase was sometimes observed and could produce several acoustic pulses.

One set of scaling issues arises because the ratio of the cavitation nuclei size to the headform size changes as the headform diameter changes. The other set of scaling issues derives from the complex interactions between the bubbles and the flow close to the headform with which the bubbles interact. Since the flow is Reynolds number dependent, scaling effects will also be caused by the changes in both body size and tunnel velocity. The question of stability of the bubble surface also arises and will be influenced by the Weber number.

In other papers, Kuhn de Chizelle et al. (1992a) have presented data on the size, sphericity, population density and collapse location of the traveling cavitation bubbles. Data on the surface streak attachment location for those bubbles which trigger patches was also included. The present paper will focus on the scaling of the noise produced. The signals recorded from the electrodes will help in the understanding of the dynamics of the bubble's collapse mechanism and the relationship with the produced noise.

2. EXPERIMENTAL SETUP

Large Cavitation Channel

The authors were fortunate to have the opportunity to examine some cavitation scaling effects by conducting experiments in a new facility called the Large Cavitation Channel, which has just been constructed for the David Taylor Research Center (Morgan, 1990). Briefly this facility is a very large water tunnel with a working section which is 3.05m x 3.05m in cross-section. It is capable of tunnel speeds above 15m/s and the pressure control allows operation at sufficiently low pressures in the working section to permit cavitation investigations.

Headforms

Three Schiebe headforms of diameter 5.08cm, 25.4cm and 50.8cm were machined out of solid blocks of clear lucite and were mounted in the working section as shown in figure 1. The Schiebe headform has a minimum pressure coefficient of Cp_{min}=-0.78 and is known to be quite robust to laminar flow separation. Lucite was chosen for its good acoustical match with water in addition to its electrically insulating properties.

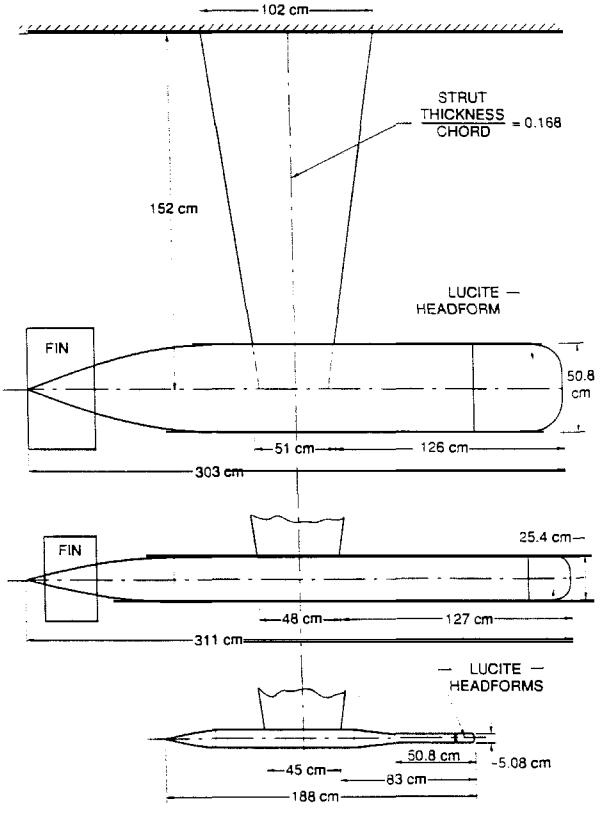

Fig. 1 Schematic diagram the three headforms with afterbodies and supporting strut.

Electrode bubble detection

Silver epoxy electrodes were installed flush in the headform. A pattern of alternating voltages is applied to the electrodes and the electric current from each is monitored. When a bubble passes over one of the electrodes, the impedance of the flow is altered, causing a drop in current (Ceccio 1989). Thirteen of these electrodes take the form of small patches (about 1mm in diameter) at different axial locations. A peak detector connected to one of the electrodes allowed detection of the presence of a traveling bubble.

High speed photography and flash

Two cameras triggered simultaneously, were set up in order to take flash pictures of individual cavitation bubbles at different angles and different enlargements. Four powerful EGG SS166 flash heads with SS162-165 energy storage racks were used. The film exposure time was of the flash duration and was measured to be about 30μs. Triggering could be done either manually or through a computer controlled lock-out system in series with the electrode peak detector signal. A delay unit was employed in order to take photographs of bubbles at various times after passing an electrode.

Hydrophones

The interiors of the headforms were hollowed out and filled with water at atmospheric pressure in order to place hydrophones as close as possible to the cavitation and provide a fairly reflection and reverberation-free acoustic path between the cavitation and the hydrophone. ITC-1042 hydrophones with a relatively flat, isotropic response out to 80kHz were used. The center of the hydrophone was placed on the axisymmetric axis, one headform radius from the front stagnation point. 64 kbyte signal acquisitions with 16 bit resolution were made at a 1MHz sampling rate. Reciprocity type calibration was performed by comparing the internal hydrophone signals with those from two STI hydrophones (with a flat frequency response up to 100kHz), installed upstream and downstream of the headform in a water filled recess in the upper wall of the working section. Using the manufacturer's response curves for the hydrophones in the receiving and transmitting modes and the theoretical transfer function of the water medium, the mean error on the reciprocity tests over the whole range of measured frequencies (from 1kHz to 100kHz) proved to be less than 3dB for all three headforms.

Test conditions

The test matrix included three saturation air contents of 80%, 50% and 30% for each of the three Schiebe headforms. The measurements were taken at three velocities of 9m/s, 11.5m/s and 15m/s, allowing a Reynolds number range from 0.54×10^6 to 9.41×10^6. For each velocity about five cavitation numbers were investigated, ranging from bubble inception to fully attached cavitation.

3. CAVITATION APPEARANCE

Inception

Cavitation inception data was described previously in Kuhn de Chizelle et al. (1992a,b) and will only be summarized here. Inception was defined as the occurrence of some minimum cavitation event rate over the entire body. The inception cavitation number was found to increase with increasing air content and headform size. For the larger headforms and 80% dissolved air content the inception cavitation number was extremely close to the $-Cp_{min}=0.78$ value. Naturally, higher cavitation numbers did not result in any events. For later reference it is important to observe that when the pressure is sufficiently low for the smallest headform to reach inception, the larger headforms already exhibit extensive cavitation patterns. The interesting range of cavitation numbers therefore varies considerably from one headform to another.

Bubble shape

For cavitation numbers close to the minimum pressure coefficient, $-Cp_{min}=0.78$, the bubble life-time is extremely short. Under these conditions they all assume a very thin disk-like geometry and there is little or no growth normal to the headform surface due to the high normal pressure gradients.

As the cavitation number is decreased below inception, the bubbles grow in volume (in diameter and in height) and adopt the hemispherical cap shape seen in photograph 2a. One entirely new observation from the current experiments was of the presence of wave-like circular dimples on the top of the bubble (figures 2a, 2b). These were not seen on the 5.08cm headform and seem to become more pronounced as the volume of the bubble increases. This effect may be Weber number dependent. The dimples seem quite stable, and remain on the bubble until the very last stage of collapse.

Observations of bubbles on all three headforms show that the maximum radius of

the base of the hemispherical cap, R, scales linearly with the headform diameter, D (Kuhn de Chizelle et al., 1992a) and appears to be mostly cavitation number dependent.

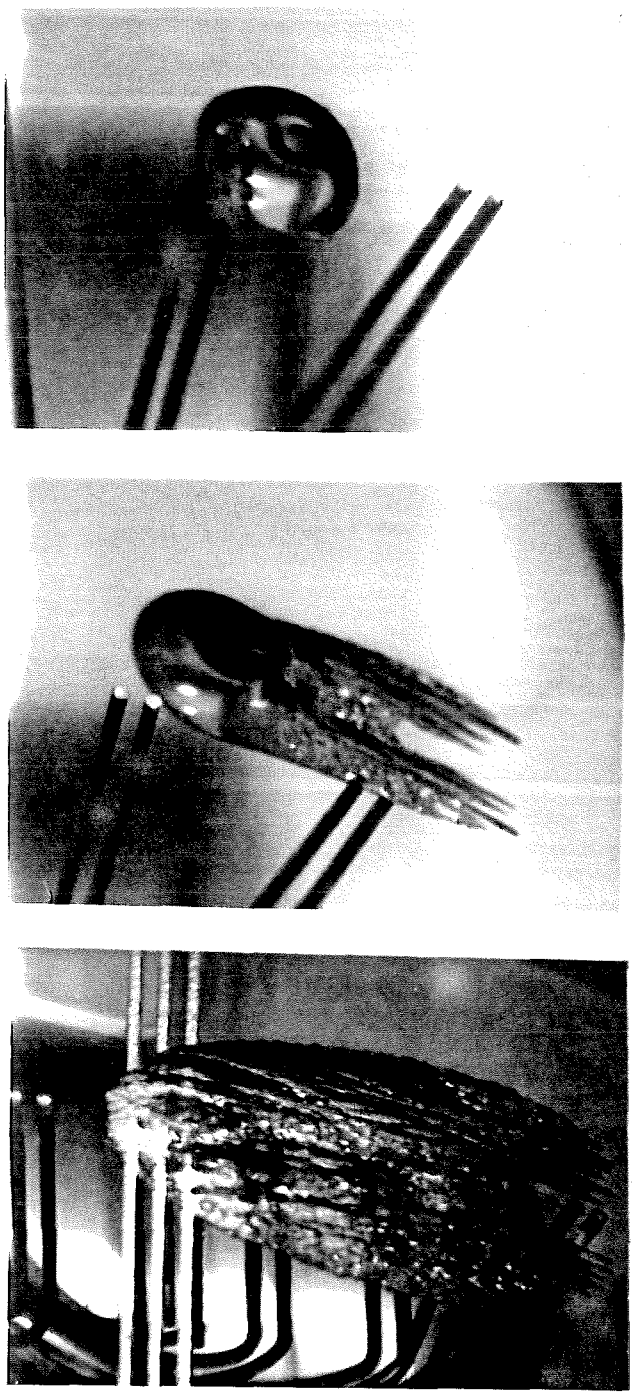

Fig. 2 High speed photography of cavitation events taken on the 50.8cm diameter headform at 30% saturation dissolved air content (distance between the two pairs of patch electrodes: 2.54cm). Figures **a,b**: U_o=15m/s, σ=0.60; Figure **c**: U_o=15m/s, σ=0.55

Bubble streaks and patches

At lower cavitation numbers and on the larger headforms many of the individual bubbles produce streaks of cavitation which are "attached" to the headform at their upstream end and are stretched and grow as the bubble moves downstream (see figure 2b). In the present experiments the frequency of occurrence of attached streaks increased with velocity and headform size (increased Reynolds number) and with decreasing cavitation number. For small enough cavitation numbers the patch can out-grow the bubble, leaving behind large transient patch-like cavities as shown in photograph 2.

Bubble-patch interactions

When the cavitation number is sufficiently small, the transient patches become fairly stable and remain on the headform, thus creating attached cavities for periods of up to a few seconds. As their number increases the patches will merge to create larger attached structures.

For the larger headforms at cavitation numbers below 0.7 the two different kinds of cavitation patterns, namely traveling bubbles and transient attached patches would co-exist. Quite remarkably, even for the conditions at which we observe extensive, fixed patch-type cavitation, some very smooth hemispherical traveling bubbles are still present. Bubbles riding over attached cavities will eventually collapse and merge completely with the latter upstream of its closure region. As will be shown further in this paper, these interactions greatly affect the noise generation.

4. CAVITATION NOISE

Averaged bubble noise

For a range of cavitation numbers between inception and a value at which the cavitation patches persisted, it was possible to identify in the hydrophone output the signal produced by an individual bubble collapse. It was found necessary to digitally high pass filter the signals using a cut-off frequency of 5kHz in order to reduce the effect of vibration and noise caused by cavitation at the top of the

supporting strut. This filtering did not, however, substantially effect the results. Secondly the processing amplifier gain response was calibrated and applied to the results.

FFT analyses of the signals from individual events were performed for different cavitation conditions for Nyquist frequencies up to 500kHz. In order to compare the shape of the power spectral density for different cavitating conditions the values have been non-dimensionalized by the number of sampled points, N, times the mean squared power amplitude, $\overline{PSD}$, where

$$\overline{PSD} = \frac{1}{N^2}\left[C^2(f_0) + C^2(f_{N/2}) + 2\sum_{i=1}^{i=N/2-1} C^2(f_i)\right].$$

The dimensionless PSD curves shown in figure 3 are data averaged over several cavitation events.

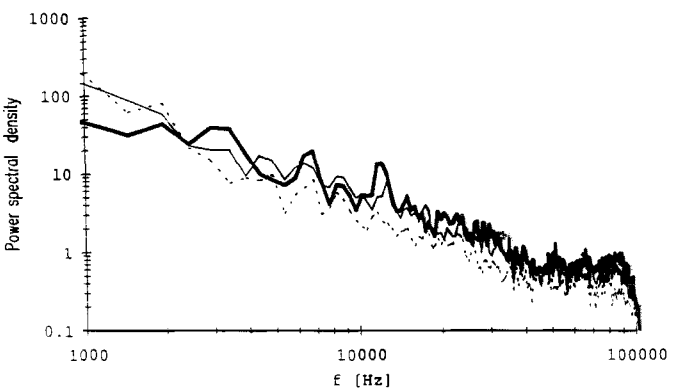

Fig. 3 Averaged dimensionless power spectral density signals for the 50.8cm headform: ——— U_o=9m/s σ=0.66; ——— U_o=11.5m/s σ=0.64; ------- U_o=15m/s σ=0.61

First we notice that for all headforms and tests conditions the measured spectral shape varies little with operating cavitation conditions close to inception. The influence of the hydrophone cutoff frequency above 80kHz can be observed in all signals. Asymptotic analysis of the Rayleigh-Plesset equation predicts a power spectral decay of -16dB/decade for frequencies of 10kHz to 100kHz. The measured decay between 1kHz and 80kHz in the present data appears roughly constant, with a value of about -22dB/dec for all conditions. This value is similar to the value of -24dB/dec obtained earlier by Ceccio and Brennen (1990) and by Kumar and Brennen (1991) in the Caltech Low Turbulence Water Tunnel.

Measurements of the frequency decay as a function of the cavitation number for different cavitating conditions are shown in figure 4. We observe that this slope seems to decrease as the cavitation number value is reduced below 0.6. For some cavitation conditions the slope can be as low as -35dB/dec.

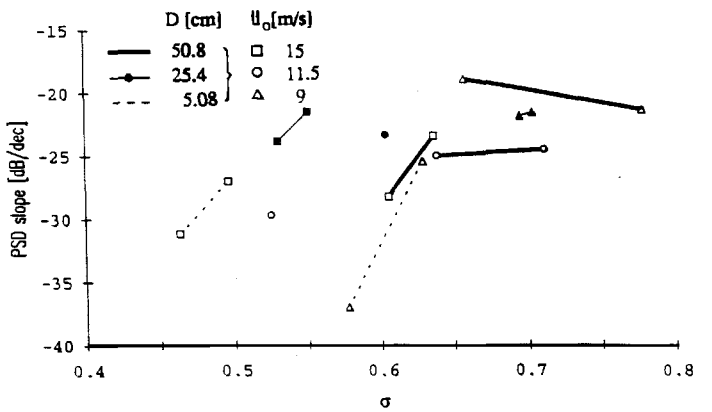

Fig 4. Average power spectral density slope decay between 1kHz and 80kHz [dB/dec]. Measurements for different headform diameters and velocities as a function of the cavitation number.

The amplitudes of the acoustic pressure pulses were measured by defining the impulse, I, as the integral under the instantaneous pressure time history from the beginning of the collapse pulse to the moment when the pressure returns to its mean value. Since the impulse will vary inversely with the distance of the hydrophone from the noise source, we divide I by the appropriate headform radius and form a dimensionless impulse, I*, by dividing by the free stream velocity and the fluid density as indicated by the Rayleigh-

Plesset analysis, so that $I^* = 8\pi I/\rho D U_o$. The hydrophone output for each of the experimental conditions was examined in order to identify at least 40 of the larger pulses associated with a bubble collapse. The average values of the non-dimensional impulses obtained in this way are plotted against cavitation number in figure 5.

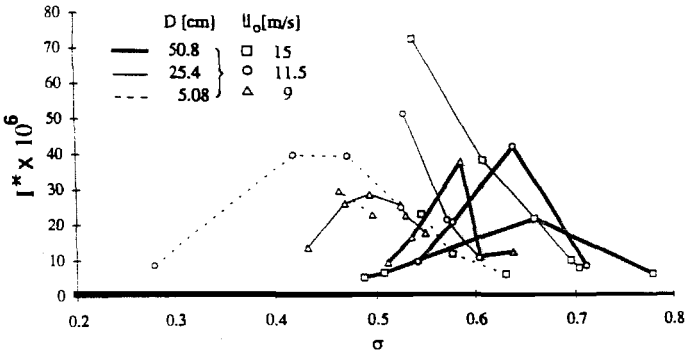

Fig. 5 Average dimensionless maximum acoustic impulse, I*, for all three headforms as a function of the cavitation number.

The non-dimensional impulse is of the same order of magnitude for all three headforms. It initially increases as the cavitation number is decreased below inception. However most of the data also indicates that the maximum impulse ceases to increase and, in fact, decreases when σ is decreased below a certain value (about 0.43, 0.50 and 0.62 for the 5.08cm 25.4cm and 50.8cm diameter headform). The decrease at low cavitation numbers could be explained by the increasing presence of attached cavitation patches, damping the bubble collapse mechanism. The location of the peaks appears to be somewhat influenced by the velocity: they are shifted towards higher cavitation numbers for lower velocities. This trend is consistent with previous observations (Kuhn de Chizelle et al., 1992a) of the average void fraction over the headform at constant cavitation numbers, which exhibited an increase with a decrease in velocity. The conditions at which the impulses, I*, are maximum seem to correspond to circumstances in which the cavities cover about 20% of the surface area of the headform in the neighborhood of the minimum pressure point. Higher void fractions increase the interactions between the bubbles and the patches and considerably reduce the acoustic impulse. Such an effect was also previously reported by Arakeri and Shanmuganathan (1985). It is important to note that the results presented here correspond to averaged values, and that the standard deviation of these impulses is about 40% of the average value. Therefore for identical cavitation conditions the cavitation noise may vary considerably from one event to another.

In summary, we find that the acoustic impulse produced by a single bubble collapse, while exhibiting considerable variability, nevertheless scales with headform size and tunnel velocity in the way which is expected on the basis of the Rayleigh-Plesset analysis. Moreover, when the bubble concentration exceeeds a certain value the noise from individual events becomes attenuated.

5. CONCLUSIONS

The present experiments first revealed substantially lower cavitation inception numbers for the larger headforms. At bubble inception conditions on the smallest headform we observed fully developed attached cavitation on the largest. The most noticeable effect of scale on the appearance of cavitation was the increase in bubble-generated attached streaks and patches for the larger headforms. On the 5.08cm headform a traveling bubble would occasionally generate two attached streaks or tails at the lateral extremes of the bubble. These would disappear almost immediately after the bubble collapsed. On the larger headforms at higher speeds (larger Reynolds numbers) and low cavitation numbers the streaks began to occur more frequently and extend behind the entire width of the bubble. The streaks would tend to produce a transient patch of attached cavitation which would disappear as the bubble collapsed. We saw that the pressure impulse could be adequately scaled with the headform diameter and the free stream

velocity, in agreement with the Rayleigh-Plesset analysis. As expected, lower cavitation numbers lead to higher impulses as long as the interference with larger patch type cavities remained limited. The shearing mechanism of individual bubbles, producing trailing streaks and patch cavities greatly decreased the emitted collapse noise. Finally there appears to be a bubble interaction effect when the cavity coverage on the surface of the headform exceeds about 20% which tends to decrease the cavitation noise.

ACKNOWLEDGMENTS

Large scale experiments like these require help of many people and the authors are very grateful to all of those who helped in this enterprise. We are very grateful to the ONR for their support under contracts N00014-91-J-1426 (SLC) and N00014-91-J-1295 (CEB, YKdC). We are also extremely grateful to the David Taylor Research Center (DTRC) and to their staff including W.B. Morgan for making the use of the LCC possible for us and to both Scott Gowing and James Blanton. Po-Wen Yu from the U. of Michigan also provided important help with the photography.

REFERENCES

Arakeri, V.H. and Shanmuganathan, V. 1985. *On the evidence for the effect of bubble interference on cavitation noise.* J. Fluid Mech., Vol. 159, pp. 131-150.

Brennen, C.E. and Ceccio, S.L. 1989. *Recent Observations on cavitation and cavitation noise.* Proc. ASME Third Int. Symp. on Cavitation Noise and Erosion in Fluid Systems, San Francisco, FED-Vol. 88, pp. 67-78.

Blake, W.K., Wolpert, M.J. and Geib, F.E. 1977. *Cavitation noise and inception as influenced by boundary layer development on a hydrofoil.* J. Fluid Mech., Vol. 80, pp. 617-640.

Ceccio, S.L. and Brennen, C.E. 1991. *The dynamics and acoustics of traveling bubble cavitation.* J. Fluid Mech., Vol. 233, pp. 633-660.

D'Agostino, L., Brennen, C.E. and Acosta, A.J. 1988. *Linearized dynamics of two-dimensional bubbly and cavitating flows over slender surfaces.* J. Fluid Mech., Vol. 192, pp. 485-509.

Fitzpatrick, H.M. and Strasberg, M. 1956. *Hydrodynamic sources of sound.* First Symp. on Naval Hydrodynamics, Washington D.C., pp. 241-280.

Kuhn de Chizelle, Y., Ceccio, S.L., Brennen, C.E. and Shen, Y. 1992 (a). *Cavitation scaling experiments with headforms: Bubble dynamics.* Proc. Second International Symposium on Propeller and Cavitation ISPC, Hangzhou, China.

Kuhn de Chizelle, Y., Ceccio, S.L., Brennen, C.E. and Shen, Y. 1992 (b). *Scaling experiments on the dynamics and acoustics of traveling bubble cavitation.* Proc. Institution of Mechanical Engineers, Cambridge, UK.

Kumar, S. and Brennen, C.E. 1991. *Statistics of noise generated by traveling bubble cavitation.* ASME Cavitation and Multiphase Flow Forum, Portland OR, June 1991, FED Vol. 109, pp. 55-62.

Kumar, S. and Brennen, C.E. 1992. *An acoustical study of traveling bubble cavitation.* Submitted to J. of Fluid Mech.

Lindgren, H. and Johnsson, C.A. 1966. *Cavitation inception on headforms. ITTC comparative experiments.* 11th Int. Towing Tank Conf., pp. 219-232.

Meyer, R.S., Billet, M.L. and Holl, J.W. 1989. *Free-stream nuclei and cavitation.* Proc. ASME Third Int. Symp. on Cavitation Noise and Erosion in Fluid Systems, San Francisco, FED-Vol. 88, pp. 52-62.

Morgan, W.B. 1990. *David Taylor Research Center's Large Cavitation Channel.* Proc. Int. Towing Tank Conference, Madrid, Spain, pp. 1-9.

Schiebe, F.R. 1972. *Measurements of the cavitation susceptibility of water using standard bodies.* St. Anthony Falls Hydraulic Lab., Univ. of Minnesota, Rep. No. 118.

Vogel, A., Lauterborn, W. and Timm, R. 1989. *Optical and acoustic investigations of dynamics of the Laser-produced cavitation bubbles near a solid boundary layer.* J. Fluid Mech., Vol. 206, pp. 299-338.